NANO LETTERS

2005
Vol. 5, No. 3
425−428

Self-Assembly of Concentric Quantum Double Rings

Takaaki Mano,*,† Takashi Kuroda,†,‡ Stefano Sanguinetti,†,§ Tetsuyuki Ochiai,† Takahiro Tateno,† Jongsu Kim,† Takeshi Noda,† Mitsuo Kawabe,† Kazuaki Sakoda,† Giyuu Kido,† and Nobuyuki Koguchi†

Nanomaterials Laboratory, National Institute for Materials Science, 1-2-1 Sengen, Tsukuba, Ibaraki 305-0047, Japan, PRESTO, Japan Science and Technology Agency, 4-1-8 Honcho-Kawaguchi 331-0012, Japan, and I.N.F.M. and Dipartimento di Scienza dei Materiali, Universitá di Milano Bicocca, Via Cozzi, I-20125 Milano, Italy

Received November 2, 2004; Revised Manuscript Received January 16, 2005

ABSTRACT

We demonstrate the self-assembled formation of concentric quantum double rings with high uniformity and excellent rotational symmetry using the droplet epitaxy technique. Varying the growth process conditions can control each ring's size. Photoluminescence spectra emitted from an individual quantum ring complex show peculiar quantized levels that are specified by the carriers' orbital trajectories.

Physical properties of materials are governed by their electronic states, which are, in turn, determined by the microscopic configuration of their constituent atoms. Recent development of nanofabrication technology allows us to create and assemble atomic units in an artificial manner, such as in the fabrication of quantum dots,[1−4] molecule-like alignment of two quantum dots,[5,6] and the formation of a nanometer-sized ring cluster (quantum ring), which is an artificial benzene analogue.[7,8] To extend such a bottom-up approach to the study of complicated systems such as cross-linked molecules, we must establish a procedure for nano-structural assembly. This letter reports the formation and characterization of quantum ring complexes. Using droplet epitaxy technique, we performed self-assembly of concentric quantum double rings with high uniformity and excellent rotational symmetry. These ring complexes open a new route, promised by ring geometry, to measurement of quantum interference effects.[9,10]

We have realized quantum ring complexes by droplet epitaxy, an epitaxial growth method. That method has a high potential for fabrication of semiconductor nanostructures in lattice-matched systems[2] such as GaAs/(Al,Ga)As.[11,12] In this technique, gallium (Ga) molecular beams are supplied initially without arsenic (As) ambience, leading to the formation of droplet-like clusters of Ga atoms on the substrate. After droplet formation, an As flux is supplied in the chamber, thereby crystallizing the droplets into GaAs nanocrystals. Our previous works have reported the formation of quantum dots with excellent control of densities and sizes.[12] Because the crystalline morphology is governed by the interplay between the migration of surface adatoms and their crystallization, we can also control the shape of nanocrystals by varying the condition of this process.

Atomic force microscope (AFM) images of the nanocrystals at various stages of growth are displayed in Figure 1. By supplying Ga atoms to the $Al_{0.3}Ga_{0.7}As$ surface, droplets of Ga atoms with hemispherical shape are formed (Figure 1a). When these droplets are irradiated with an As flux of sufficiently high intensity (2×10^{-4} Torr beam equivalent pressure (BEP)), they become cone-like nanocrystals of GaAs.[12] Reduction of the As flux, roughly by a factor of 100, alters the nanocrystal morphology completely to unique "concentric double rings", which are composed of split inner and outer rings with a well-defined central hole (Figure 1b). The respective diameters of the inner and outer rings are 45 (± 3) nm and 100 (± 5) nm; both rings are 3 (± 1) nm high. The rings show a good circular symmetry, with slight elongation along the [0−11] direction (less than 5% for the inner ring and 8% for the outer ring) (Figure 1c). Figure 2 shows the configuration of the concentric double rings with a high-resolution scanning electron microscope (HR−SEM) image.

Dependence of the nanocrystal shape on the intensity of As flux implies some possible formation mechanisms of such concentric double-ring structures. Cross-sectional profiles of a series of nanocrystals, obtained by subjecting the Ga droplets to different As flux, are presented in Figure 3.

* Corresponding author. E-mail: MANO.Takaaki@nims.go.jp, Phone: +81-29-859-2790, Fax: +81-29-859-2701.
† Nanomaterials Laboratory, National Institute for Materials Science.
‡ PRESTO, Japan Science and Technology Agency (JST).
§ I.N.F.M. and Dipartimento di Scienza dei Materiali, Universitá di Milano Bicocca.

10.1021/nl048192+ CCC: $30.25
Published on Web 02/08/2005

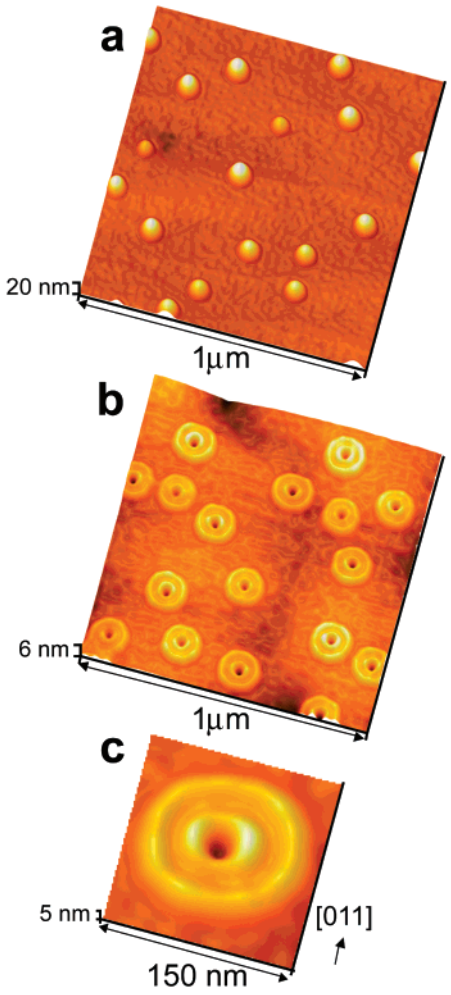

Figure 1. Atomic force microscope (AFM) surface images. The samples were grown on GaAs (100) substrates using solid-source molecular beam epitaxy. (a) Gallium (Ga) droplets with the density of 2×10^9 cm^{-2} were formed using a supply of 3.75 monolayer (ML) of Ga (0.5 ML/s) to the surface of a $Al_{0.3}Ga_{0.7}As$ barrier layer at 300 °C. (b) GaAs "concentric double rings", formed using a supply of arsenic (As) flux (As_4 molecular beam) with intensity of 2×10^{-6} Torr beam equivalent pressure (BEP) to the Ga droplets at 200 °C. (c) Magnified image of the single "concentric double rings".

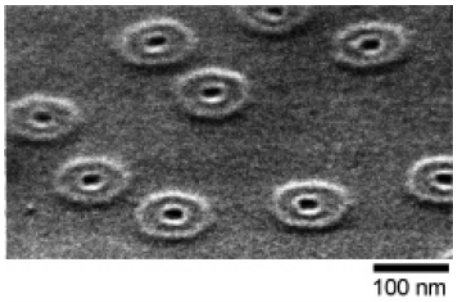

Figure 2. High-resolution scanning electron microscope (HR−SEM) image of the GaAs/$Al_{0.3}Ga_{0.7}As$ concentric double rings. The same sample as that of Figure 1b is shown here.

Through this experimental series, we prepared Ga droplets made with identical growth conditions to those indicated in Figure 3a. When we apply an intense As flux to the droplet,

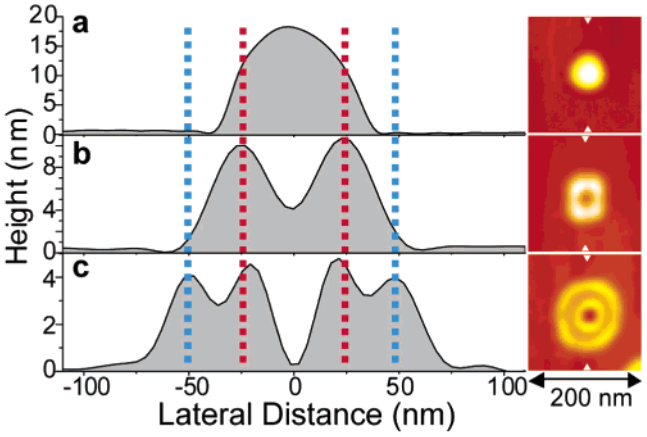

Figure 3. Cross-section profiles along the [0−11] direction (indicated by white arrowheads in the right-hand side of atomic force microscope (AFM) images). (a) Gallium (Ga) droplet, formed using a supply of a 3.75 monolayer (ML) of Ga to the surface of $Al_{0.3}Ga_{0.7}As$ barrier layer at 350 °C. (b) GaAs "single" ring, formed using a supply of arsenic (As) flux with intensity of 8×10^{-6} Torr beam equivalent pressure (BEP) to the Ga droplets at 200 °C. (c) GaAs "concentric double rings", formed using a supply of As flux with intensity of 2×10^{-6} Torr BEP to the Ga droplets at 200 °C.

the shape of the formed nanocrystals simply follows that of the original Ga droplet.[12] By decreasing the As flux 1 order of magnitude, the nanocrystals evolve into a ring-like shape,[13] as shown in Figure 3b. The lateral size of the ring, denoted by the red-dotted lines, is almost identical to that of the original Ga droplet; it changes with the droplet size.[13] These findings suggest that more effective crystallization occurs at the droplet boundaries,[14] where the Ga atoms (from the droplets) react frequently with the As atoms (from the molecular flux), engendering the formation of the ring-like nanocrystals.

When we decrease the As flux intensity further to a quarter that of the "single" ring formation, the mean height of nanocrystals decreases. In addition, another ring appears, forming a concentric double-ring structure (Figure 3c). The inner ring diameter is almost identical to that of the "single" ring mentioned previously; the outer ring is formed outside that ring. It must be emphasized that the volume of each nanocrystal is unchanged for different As flux. By averaging crystalline volume through AFM analysis, we can estimate the atomic quantity inside a Ga droplet (Figure 3a) to be on the order of 10^6.[16] After crystallization into GaAs, both single rings and concentric double rings are found to consist of 1.5×10^6 atoms, showing fairly good agreement with that of the original droplet. Therefore, we confirm that all Ga atoms are crystallized into GaAs. The final crystalline shape depends on the As flux intensity.

We should note that the outer ring diameter, denoted by the blue-dotted lines, becomes greater than the diameter of the original Ga droplet. This fact indicates the migration of Ga atoms away from the droplet. In the crystallization stage, Ga atoms are mainly within the droplets; As atoms are densely dispersed on the surface far from the droplet. This concentration gradient might engender migration of Ga atoms away from the droplet, and that of the As atoms toward the droplet. Efficient counter flows of Ga and As atoms result

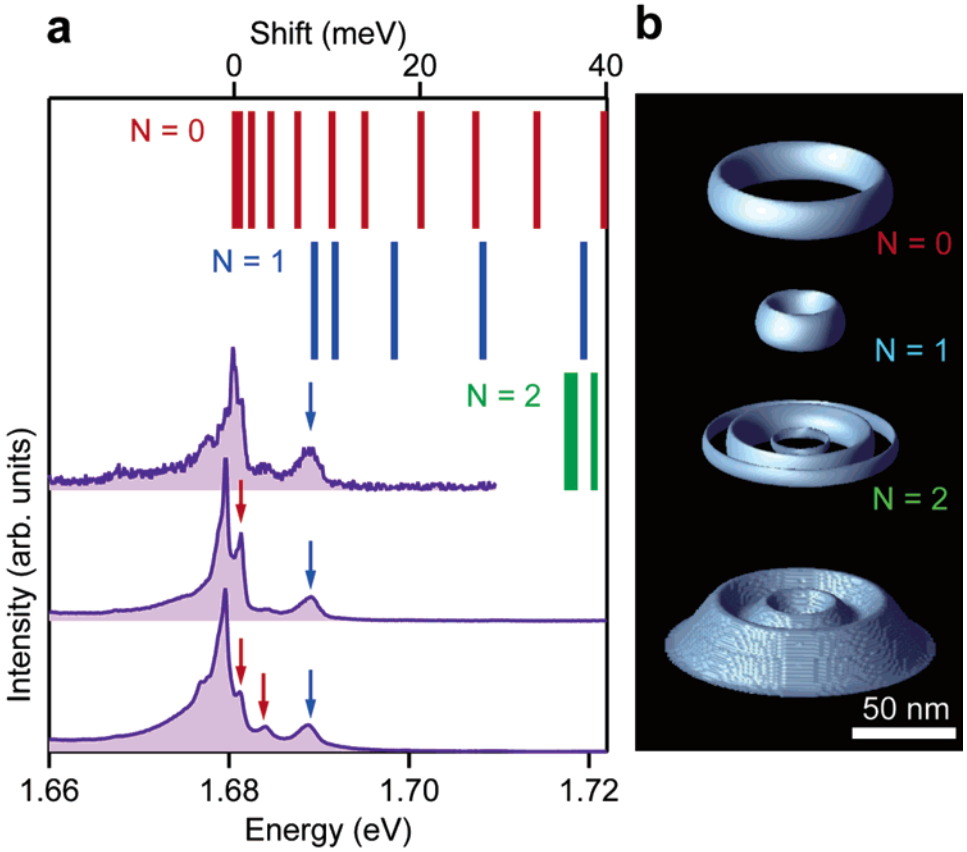

Figure 4. Energy states of the concentric double rings. (a) PL of a single quantum concentric double ring structure (bottom) and the calculated energy shift with respect to the ground-state emission (top). The respective excitation intensities were, from top to bottom, 1, 10, and 30 W/cm^2. Spectra are normalized to their maxima and offset for clarity. At the top, red, blue, and green lines respectively represent the calculated energies of the optical transition of $N = 0$, $N = 1$, and $N = 2$ series with various angular momenta. The energy split in the PL from the main peak to the high-energy satellite (indicated by a blue arrow) agrees with the calculated energy shift between the transitions with $(N, J) = (0, 0)$ and $(N, J) = (1, 0)$. In the PL spectra at high injection, small contributions associated with transitions of higher angular momenta ($J > 0$) are also shown (red arrows). (b) Isosurface plots of the electronic probability density at 50% of the maxima in the concentric quantum double rings. From top to bottom, these panels show the wave function of the ground state ($N = 0$), that of the first excited radial state ($N = 1$) with $J = 0$, that of $N = 2$ ($J = 0$), and the potential profile used for calculation.

in the crystallization of GaAs outside the original droplet, i.e., outer ring formation. This interpretation is supported by the fact that the outer ring diameter increases with decreasing As flux intensity, whereas that of the inner ring remains almost unchanged.[17] For more detailed elucidation of the growth mechanism, however, further studies are necessary.

We performed photoluminescence (PL) measurements on single quantum ring complexes to characterize the electronic structure and to assess their quantum confinement capability. For that purpose, we prepared the concentric double rings with density down to 1.3×10^8 cm^{-2} and capped by an $Al_{0.3}Ga_{0.7}As$ barrier layer followed by rapid thermal annealing (750 °C for 4 min).[13,15] The combination of the low-density sample and a micro-objective setup allowed us to isolate a single nanocrystal from the emission signal. The PL spectra, measured at increasing power excitation intensity, are presented in the bottom part of Figure 4a. At low excitation intensity (1 W/cm^2), the PL consists of an intense peak at 1.68 eV, with a satellite peak located at 8 meV on the high-energy side (indicated by a blue arrow). Other minor contributions are present on the high-energy side of the main peak (indicated by red arrows), whose intensity increases with the excitation density. With increasing illumination, line broadening, associated with the scattering of carriers, and spectral red shift of the emission, which reflects multiple-carrier effects, were observed. It must be emphasized that such PL characteristics are common to all measured concentric double-ring structures, even though the centroid energy may vary (within a few tens of meV) because of a certain size distribution of the structures.

To assign the observed PL features, we calculated the electronic energy levels within effective mass approximation.[18−20] For computational purposes, we assume that the quantum rings have a rotational symmetry along the growth axis. Aside from this assumption, no adjustable parameters are used in the model. The average shape, as determined by AFM measurements, was adopted as the confinement potential for electrons (e) and holes (h). Material parameters for $GaAs/Al_{0.3}Ga_{0.7}As$ at 4 K[21,22] are summarized in Table 1. Within this framework, we consider the quantized motion of two-dimensional degrees of freedom: the radial motion, as specified by the principal quantum number N, and the rotational motion, as specified by the angular momentum (rotational quantum number) J. Dominant contributions to the optical transition occur from the recombination of e and

Table 1. Material Parameters Used in the Effective-Mass Calculation for the Band Alignments of the Conduction Band (CB) and the Valence Band (VB)

quantity	unit	GaAs	$Al_{0.3}Ga_{0.7}As$
CB effective mass[21]	m_0	0.067	0.093
VB effective mass (heavy hole)[21]	m_0	0.51	0.57
CB band mismatch[22]	meV	262	
VB band mismatch[22]	meV	195	

h, characterized by the same quantum numbers. As a matter of fact, the optical transitions connecting e and h with different quantum numbers have oscillator strengths at least 1 order of magnitude lower than that connecting e and h states with the same quantum numbers. Consequently, hereafter, the relevant e-h transitions to be connected with PL lines will be indicated using only a single pair of N and J numbers.

At the top part of Figure 4a, we present energies of the calculated principal optical transitions. The electronic wave functions corresponding to these states are illustrated in Figure 4b, showing the electron in the ground state ($N = 0$) as confined in the outer ring, whereas that of the excited state in radial motion ($N = 1$) is confined in the inner ring. The higher excited state ($N = 2$) lies in both rings, with a p-like wave function in the outer ring. We find excellent agreement between the calculated transition energy and the PL spectra. The two distinct peaks in the PL (the main peak and the higher-energy satellite, observed at low injection) are interpreted in terms of transitions between e and h in the ground state, (N, J) = (0, 0); thus they are emitted from the outer ring, and the first excited radial state, (N, J) = (1, 0), therefore coming from the inner ring. The shoulder, occurring at high injection and observed on the high-energy side of the main peak, is assigned to a multiplet involving several transitions at large angular momenta, $J > 0$, of the ground radial state. It reflects the state filling caused by photoinjected carriers. Because of the small overlap between the $N = 0$ and the $N = 1$ states, the relevant relaxation associated with the carrier transfer from the inner ring to the outer ring is inferred to be ineffective. We can estimate the population of carriers in the PL experiments at the lowest excitation intensity as less than 0.1 on the basis of the carrier capture cross-section as determined from similar nanostructures.[23] Therefore, the presence of excited-state emission at low excitation reflects the quench of carrier relaxation between the excited and ground radial states.

In conclusion, we found the self-assembly of semiconductor ring complexes at the nanoscale. By varying the conditions of droplet epitaxial growth, a drastic change of the microcrystalline shape, from dots to single rings and to concentric double rings, was observed. Emission spectra revealed the formation of characteristic electronic states in the concentric double rings.

Acknowledgment. We are grateful to M. Yamagiwa, Y. Imanaka, T. Takamasu, and T. Yakabe for their fruitful discussions. We thank K. Yoshihara who encouraged us in our research. T.K. acknowledges support of a Grant-in-Aid from MEXT (15710076).

References

(1) Bimberg, D.; Grundman, M.; Ledentsov, N. N. *Quantum Dot Heterostructures*; John Wiley & Sons Ltd.: Chichester, 1999.
(2) Koguchi, N.; Takahashi, S.; Chikyow, T. *J. Cryst. Growth* **1991**, *111*(1−4), 688.
(3) Leonard, D.; Krishnamurthy, M.; Reaves, C. M.; Denbaars, S. P.; Petroff, P. M. *Appl. Phys. Lett.* **1993**, *63*(23), 3203.
(4) Banin, U.; Cao, Y.; Katz, D.; Millo, O. *Nature* **1999**, *400*(6744), 542.
(5) van der Vaart, N. C.; Godijn, S. F.; Nazarov, Y. V.; Harmans, C. J. P. M.; Mooij, J. E.; Molenkamp, L. W.; Foxon, C. T. *Phys. Rev. Lett.* **1995**, *74*(23), 4702.
(6) Bayer, M.; Hawrylak, P.; Hinzer, K.; Fafard, S.; Korkusinski, M.; Wasilewski, Z. R.; Stern, O.; Forchel, A. *Science* **2001**, *291*(5503), 451.
(7) García, J. M.; Medeiros-Ribeiro, G.; Schmidt, K.; Ngo, T.; Feng, J. L.; Lorke, A.; Kotthaus, J.; Petroff, P. M. *Appl. Phys. Lett.* **1997**, *71*(14), 2014.
(8) Lorke, A.; Johannes Luyken, R.; Govorov, A. O.; Kotthaus, J. P.; Garcia, J. M.; Petroff, P. M. *Phys. Rev. Lett.* **2000**, *84*(10), 2223.
(9) Berry, M. V. *Proc. R. Soc. London, Ser. A* **1984**, *392*, 45.
(10) Shapere, A.; Wilczek, F. *Geometric Phases in Physics*; Advanced Series in Mathematical Physics, Vol. 5; World Scientific Pub. Co. Inc.: Singapore, 1988.
(11) Koguchi, N.; Ishige, K. *Jpn. J. Appl. Phys.* **1993**, *32*(5A), 2052.
(12) Watanabe, K.; Koguchi, N.; Gotoh, Y. *Jpn. J. Appl. Phys.* **2000**, *39*(2A), L79.
(13) Mano, T.; Koguchi, N. Nanometer-scale GaAs ring structure grown by droplet epitaxy. *J. Cryst. Growth*, in press.
(14) Mano, T.; Watanabe, K.; Tsukamoto, S.; Fujioka, H.; Oshima, M.; Koguchi, N. *J. Cryst. Growth* **2000**, *209*(2−3), 504.
(15) Watanabe, K.; Tsukamoto, S.; Gotoh, Y.; Koguchi, N. *J. Cryst. Growth* **2001**, *227−228*, 1073.
(16) Because of the large aspect ratio of the droplet, the lateral size of the AFM image (Figure 3a) is slightly greater than that of the real shape. We assume its shape to be hemispherical with a contact angle of 70° to estimate the droplet volume. See ref 11.
(17) Mano, T.; Koguchi, N., unpublished.
(18) Marzin, J. Y.; Bastard, G. *Solid State Commun.* **1994**, *92*(5), 437.
(19) Califano, M.; Harrison, P. *Phys. Rev. B* **2000**, *61*(16), 10959.
(20) Sanguinetti, S.; Watanabe, K.; Kuroda, T.; Minami, F.; Gotoh, Y.; Koguchi, N. *J. Cryst. Growth* **2002**, *242*(3−4), 321.
(21) Pavesi, L.; Guzzi, M. *J. Appl. Phys.* **1994**, *75*, 4779.
(22) Yamagiwa, M.; Sumita, N.; Minami, F.; Koguchi, N. *J. Lumin.* **2004**, *108*(1−4), 379.
(23) Kuroda, T.; Sanguinetti, S.; Gurioli, M.; Watanabe, K.; Minami, F.; Koguchi, N. *Phys. Rev. B* **2002**, *66*, 121302(R).

NL048192+